Acta Crystallographica Section D
Biological Crystallography
ISSN 0907-4449

Structural basis for a hand-like site in the calcium sensor CatchER with fast kinetics

Ying Zhang,[a] Florence Reddish,[a] Shen Tang,[a] You Zhuo,[a] Yuan-Fang Wang,[b] Jenny J. Yang[a,c] and Irene T. Weber[a,b,c]*

[a]Department of Chemistry, Georgia State University, Atlanta, GA 30303, USA, [b]Depart-Department of Biology, Georgia State University, Atlanta, GA 30303, USA, and [c]Centre for Diagnostics and Therapeutics, Georgia State University, Atlanta, GA 30303, USA

Correspondence e-mail: iweber@gsu.edu

Received 4 June 2013
Accepted 30 July 2013

PDB References: CatchER-Gd^{3+}, 4l12; CatchER(apo), 4l13; CatchER-Ca^{2+}, 4l1i

Calcium ions, which are important signaling molecules, can be detected in the endoplasmic reticulum by an engineered mutant of green fluorescent protein (GFP) designated CatchER with a fast off-rate. High resolution (1.78–1.20 Å) crystal structures were analyzed for CatchER in the apo form and in complexes with calcium or gadolinium to probe the binding site for metal ions. While CatchER exhibits a 1:1 binding stoichiometry in solution, two positions were observed for each of the metal ions bound within the hand-like site formed by the carboxylate side chains of the mutated residues S147E, S202D, Q204E, F223E and T225E that may be responsible for its fast kinetic properties. Comparison of the structures of CatchER, wild-type GFP and enhanced GFP confirmed that different conformations of Thr203 and Glu222 are associated with the two forms of Tyr66 of the chromophore which are responsible for the absorbance wavelengths of the different proteins. Calcium binding to CatchER may shift the equilibrium for conformational population of the Glu222 side chain and lead to further changes in its optical properties.

1. Introduction

The calcium ion (Ca^{2+}) acts as a ubiquitous signaling molecule in the regulation of numerous biological functions including heartbeat, muscle contraction, cell development and proliferation (Berridge *et al.*, 1998; Bers & Guo, 2005). Ca^{2+} signals exhibit different amplitudes and durations as the ions flow between subcellular compartments. Ca^{2+} functions as a first messenger in the central nervous system and works as an extracellular ion source for postsynaptic ligand-gated channels (Berridge, 1998). The endoplasmic reticulum (ER) functions as an intracellular Ca^{2+} store and the release of ER Ca^{2+} triggers a series of biological processes *via* binding to intracellular Ca^{2+}-sensing proteins such as calmodulin (CaM) and troponin C (TnC) (Zhang & Joseph, 2001). The Ca^{2+}-signaling events are controlled by the basal ER/SR (sarcoplasmic reticulum) Ca^{2+} level, as well as the amplitude and the kinetics of Ca^{2+} release from the calcium stores. Hence, determination of the concentration of free Ca^{2+} in the ER is of extensive interest and has stimulated the development of tractable intracellular Ca^{2+} sensors.

Many efforts have been devoted to green fluorescent protein (GFP)-based Ca^{2+}-fluorescent indicators such as the cameleons (Miyawaki *et al.*, 1997, 1999), pericams (Persechini *et al.*, 1997), TN-XL (Mank *et al.*, 2006) and TN-XXL (Mank *et al.*, 2008). Their detection is based on either fluorescence resonance energy transfer (FRET) between two different GFP variants or the pH-dependent change in ionization state of the chromophore in circularly permutated GFP (Miyawaki

© 2013 International Union of Crystallography
Printed in Singapore – all rights reserved

et al., 1997; Romoser *et al.*, 1997; Nagai *et al.*, 2001; Baird *et al.*, 1999). One common property of these sensors is that they involve the insertion of naturally occurring Ca^{2+}-sensing proteins such as CaM and its target binding peptide and are capable of sensing cytosolic calcium responses in the nanomolar to micromolar range (Takahashi *et al.*, 1999; Solovyova & Verkhratsky, 2002; Tsien, 1998). Several ER/SR sensors with lower metal-binding affinities have been developed by modifying the Ca^{2+}-binding loops or the peptide-interaction surface of CaM (Ohkura *et al.*, 2005; Miyawaki *et al.*, 1997; Palmer *et al.*, 2004, 2006; Evanko & Haydon, 2005). These sensors exhibit some limitations such as off-rates which are not fast enough to detect the calcium release during action potentials. In addition, only ∼50% of the skeletal muscle cells show a response to calcium stimulation. For the FRET-pair involved sensors, their highly variable basal CFP (cyan fluorescent protein)/YFP (yellow fluorescent protein) ratio and poor signal-to-noise ratio also limit quantitative determination of calcium concentration and calcium release (Rudolf *et al.*, 2006; Jiménez-Moreno *et al.*, 2010). Therefore, there is a pressing need for new Ca^{2+} sensors targeted to cellular compartments with putative high Ca^{2+} concentration, as in the ER/SR, to overcome these limitations. In a previous attempt to meet this urgent need, our laboratory engineered a Ca^{2+} sensor, 'G1', by grafting an EF-hand motif into enhanced green fluorescent protein (EGFP; Zou *et al.*, 2007). Unlike GFP, which can be excited at 395 and 475 nm, EGFP contains two mutations F64L and S65T and has one absorption maximum at 488 nm (Tsien, 1998; Ormö *et al.*, 1996). The F64L mutation is responsible for the improved folding efficiency at 310 K, while S65T is a critical mutation for suppressing the 395 nm absorbance peak (Tsien, 1998; Ormo *et al.*, 1996; Arpino *et al.*, 2012). This G1 sensor has an apparent K_d of 0.8 m*M* and responds to Ca^{2+} with a ratiometric fluorescence change, but with a slow kinetic response.

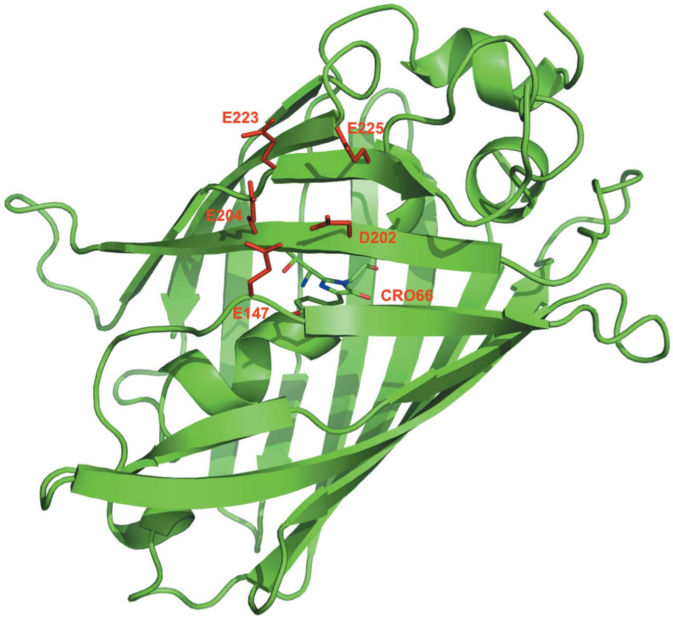

Figure 1
Structure of CatchER (green cartoon) indicating the locations of the mutated residues (red sticks) S147E, S202D, Q204E, F223E and T225E; the chromophore CRO66 is shown in green sticks with CPK atom colors.

Recently, we reported a new strategy for creating Ca^{2+} indicators by introducing a Ca^{2+}-binding site into EGFP *via* site-directed mutagenesis of selected residues in the fluorescent-sensitive location (Tang *et al.*, 2011). The single EGFP-based Ca^{2+} biosensor termed CatchER was generated by the substitutions S147E, S202D, Q204E, F223E and T225E in the designed Ca^{2+}-binding site of EGFP (Fig. 1). CatchER provides multiple advantages for reliably monitoring Ca^{2+} signaling in high [Ca^{2+}] environments. (i) It exhibits a unique calcium-induced change in optical properties. Calcium binding results in ratiometric changes in absorption, while fluorescence emission at 510 nm is increased when excited at either 398 or 490 nm (Fig. 2*a*); the high signal-to-noise ratio for fluorescent change in response to Ca^{2+} as well as the avoidance of cooperativity associated with multiple binding sites allows accurate detection of calcium both *in vitro* and *in vivo*. (ii) CatchER exhibits unprecedented dissociation kinetics, with an off-rate of >100 s^{-1} and a fast kinetic response to Ca^{2+} changes within milliseconds; recent work has also shown that CatchER is able to detect multiple calcium spikes during muscle contraction and relaxation (Wang *et al.*, 2012). (iii) The K_d of CatchER (around 1 m*M*) allows the accurate calibration of SR Ca^{2+} signaling; CatchER is able to report considerable differences in SR/ER Ca^{2+} concentration between epithelial HeLa, kidney HEK293 and muscle C2C12 cells. (iv) No invasive methods are required for CatchER detection in living organelles compared with current Ca^{2+} dyes. Such cumulative advantages, especially the fast kinetic properties, allowed us to monitor SR luminal Ca^{2+} in flexor digitorum brevis (FDB) muscle fibers to understand the mechanism of diminished SR Ca^{2+} release in aging mice (Tang *et al.*, 2011; Wang *et al.*, 2012).

In this report, we describe the crystallographic analysis of CatchER to understand the structural basis for the calcium-induced fluorescent and absorption changes and fast response. Crystal structures were determined of CatchER in the absence of Ca^{2+} [CatchER(apo)], in the presence of Ca^{2+} (CatchER-Ca^{2+}) and from crystals soaked with Gd^{3+} (CatchER-Gd^{3+}). To overcome the challenges in visualizing Ca^{2+}-binding sites in the proteins owing to the weak Ca^{2+}-binding affinity and the high off-rate and the difficulty in distinguishing calcium from water in the crystal structure, we used the heavier Gd^{3+} ions with similar metal-binding coordination properties to calcium to identify the position of the metal ion. These X-ray crystal structures of CatchER and its complexes may assist the future development of protein–ligand interaction-based biosensors for the detection of various physiological molecules.

2. Experiments and methods

2.1. Expression and purification

Protein was expressed by a modification of the procedure described in Zou *et al.* (2007). *Escherichia coli* BL21(DE3) cells transformed with pET28a vector containing the CatchER DNA were pre-cultured in 10 ml LB medium containing 6 µl

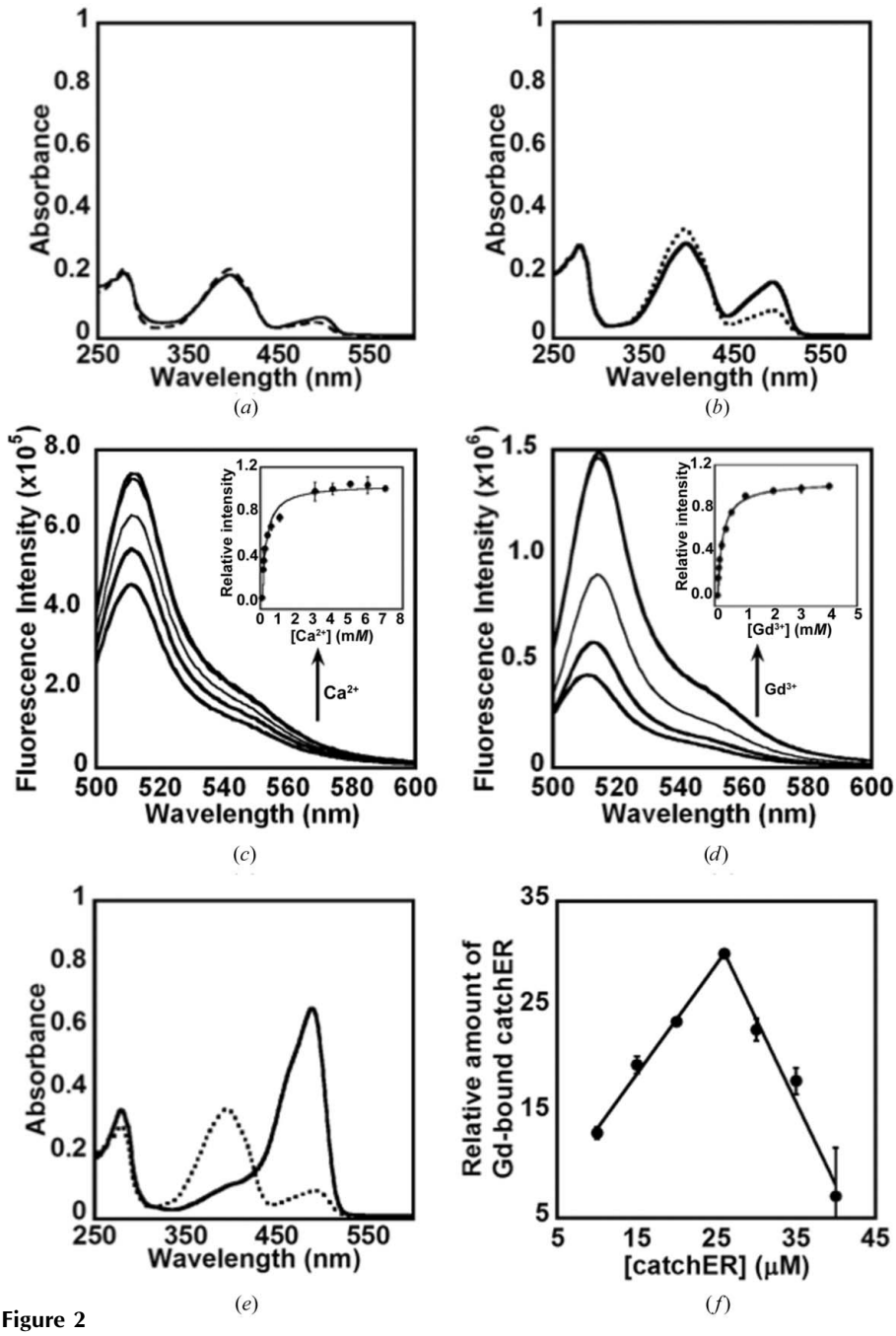

Figure 2
Absorbance spectra of CatchER and metal-binding analysis *via* fluorescence spectroscopy. (*a*) Absorbance response of CatchER to 5 m*M* Ca^{2+}: 20 µ*M* CatchER with 5 µ*M* EGTA (dashed line) in 10 m*M* Tris pH 7.4 and the same CatchER sample with 5 m*M* Ca^{2+} added (solid line). Addition of Ca^{2+} produces more of the anionic chromophore (increase in the 488 nm absorbance peak) and less of the neutral chromophore (decrease in the 395 nm absorbance peak). (*b*) Absorbance response of CatchER to 200 µ*M* Gd^{3+}. A 20 µ*M* sample of CatchER was prepared in 20 m*M* PIPES pH 6.8. The dashed line represents the sample with 5 µ*M* EGTA and the solid line is the same sample with 200 µ*M* Gd^{3+} added. (*c*, *d*) Fluorescence response of CatchER to Ca^{2+} and Gd^{3+} excited at 488 nm with emission at 510 nm with inset binding curves. The normalized fluorescence response for Ca^{2+} and Gd^{3+} was fitted with a 1:1 binding equation, producing K_d values of 227.0 ± 3.3 and 177.0 ± 13.6 µ*M* for Ca^{2+} and Gd^{3+}, respectively. (*e*) Overlay of the absorbance spectrum of 20 µ*M* CatchER with 5 µ*M* EGTA (dashed line) and 20 µ*M* EGFP (solid line) in 10 m*M* Tris pH 7.4. (*f*) Binding stoichiometry of CatchER to Gd^{3+} *via* a Job plot. The relative amount of CatchER bound to Gd^{3+} was determined using fluorescence and absorbance intensity changes in the absence and presence of Gd^{3+}. The concentrations of CatchER were 40, 35, 30, 25, 20, 15 and 10 µ*M* (the actual concentrations determined *via* the 280 nm absorbance peak were 38, 35, 30, 24, 20, 15 and 10.5 µ*M*). The total molar ratio was held constant at 50 µ*M*. The plot represents fluorescence data of complex formation from 395 nm excitation.

50 mg ml^{-1} kanamycin (30 mg ml^{-1}) and shaken overnight at 310 K. The pre-culture was transferred into 1 l Luria Bertani (LB) medium containing 30 mg ml^{-1} kanamycin and allowed to shake at 220 rev min^{-1} at 310 K until the OD reached ∼0.6, followed by the induction of protein expression by the addition of 200 µl of 1 *M* IPTG (0.2 m*M*) and a reduction in temperature to 298 K. The cells were collected by centrifugation at 7000 rev min^{-1} for 30 min at 277 K. The cell pellets were redissolved in extraction buffer (20 m*M* Tris pH 8.0, 100 m*M* NaCl, 0.1% Triton X-100) and sonicated. The cell lysate mixture was centrifuged at 17 000 rev min^{-1} and 277 K for 30 min. The supernatant was filtered using a 0.45 µm Whatman filter and the protein was purified using a 5 ml HiTrap chelating column (Amersham Biosciences, Sweden) loaded with Ni^{2+}. The protein has a six-histidine tag at the N-terminus for immobilized metal-ion affinity chromatography. High-purity fractions were concentrated to 1–2 ml and purified further using size-exclusion chromatography with a Superdex 75 100 ml column (Pharmacia Biotech) at a flow rate of 1 ml min^{-1} with 10 m*M* 4-(2-hydroxyethyl)-1-piperazineethanesulfonic acid (HEPES) buffer pH 7.4 to ensure high purity for crystallization. The 6×His tag was not removed. The protein without the tag contains 244 amino acids and has a molecular mass of ∼30 kDa.

2.2. Crystallization, X-ray data collection and structure determination

Crystals of Ca^{2+}-free and Ca^{2+}-loaded CatchER were obtained *via* the hanging-drop vapor-diffusion method using 2 µl protein solution and 2 µl reservoir solution at room temperature in 24-well VDX plates (Hampton Research, Aliso Viejo, California, USA). Ca^{2+}-free CatchER crystals (0.9 m*M* protein, 5 µ*M* EGTA) grew in a solution consisting of 51 m*M* HEPES pH 7.0, 1 m*M* β-mercaptoethanol, 50 m*M* sodium acetate, 17% PEG 4000. The Ca^{2+}-loaded CatchER complex was created by adding 50 m*M* $CaCl_2$ to 0.9 m*M* protein solution (final

Table 1
Relative amounts of CatchER-Gd^{3+} complex formation with corresponding ratios.

[CatchER] (μM)	[Gd^{3+}] (μM)	[CatchER-Gd^{3+}], absorbance at 493 nm	[CatchER-Gd^{3+}], fluorescence at 395 nm	[CatchER-Gd^{3+}], fluorescence at 488 nm	[CatchER]/[Gd^{3+}]
40	10	11.1 ± 2.3	6.7 ± 4.4	6.5 ± 3.7	4.0
35	15	18.0 ± 1.4	17.5 ± 1.2	16.4 ± 1.0	2.3
30	20	23.0 ± 0.3	22.8 ± 1.0	20.5 ± 0.7	1.5
25	25	30.8 ± 3.5	32.7 ± 0.5	20.0 ± 1.7	1.0
20	30	15.7 ± 2.2	23.6 ± 0.0	14.4 ± 0.5	0.6
15	35	10.4 ± 0.3	19.5 ± 0.8	11.4 ± 0.5	0.4
10	40	7.2 ± 0.0	13.7 ± 0.6	7.8 ± 0.3	0.2

concentration of 0.45 m*M*). Crystals of Ca^{2+}-loaded CatchER grew in mother liquor consisting of 53 m*M* HEPES pH 7.0, 1 m*M* β-mercaptoethanol, 50 m*M* sodium acetate, 16% PEG 3350. Crystals of CatchER-Gd^{3+} were obtained *via* the soaking technique. Crystals of apo CatchER were soaked for 1–2 d in a solution of mother liquor with a final concentration of 2 m*M* $GdCl_3$. The crystals were mounted in liquid nitrogen with 20%(*v*/*v*) glycerol as a cryoprotectant in the mother liquor without added metal ions. X-ray diffraction data for the crystals were collected on the SER-CAT beamline of the Advanced Photon Source, Argonne National Laboratory, Argonne, Illinois, USA. No anomalous scattering was detected for Gd^{3+} or Ca^{2+}, likely owing to the short X-ray wavelengths used.

X-ray diffraction data were processed and scaled with *HKL*-2000 (Otwinowski & Minor, 1997) and the structures were solved by molecular replacement using *MOLREP* in the *CCP*4 suite of programs (Vagin & Teplyakov, 2010; Winn *et al.*, 2011) with chain *A* of EGFP (PDB entry 2okw; Chapleau *et al.*, 2008) as the starting model. The structures of CatchER(apo) and CatchER-Gd^{3+} were refined with *REFMAC*5 (Murshudov *et al.*, 2011) and the near-atomic resolution structure of CatchER-Ca^{2+} was refined with *SHELX* (Sheldrick & Schneider, 1997; Sheldrick, 2008). Manual adjustment of the models used *Coot* v.0.5.2 (Emsley & Cowtan, 2004). The full-length protein consists of 238 amino acids; however, an N-terminal methionine was observed in these structures and was labeled residue 0 for consistency with other published GFP structures, and several C-terminal residues were not visible in the electron-density maps. In the three structures, a single protein molecule was refined with the residues labeled 0–231 in CatchER(apo) and CatchER-Gd^{3+} and 0–229 in CatchER-Ca^{2+}, while the chromophore is labeled CRO66 as in other published GFP structures. Alternate conformations were modeled for CatchER residues where observed. The solvent was modeled with waters, metal ions and other solvent molecules according to the observed electron-density maps. Anisotropic *B* factors were applied for the whole structures of CatchER-Ca^{2+} and only the Gd^{3+} atoms in CatchER-Gd^{3+}. In the CatchER-Ca^{2+} and CatchER(apo) structures residues Arg73 and Glu225 were refined with the same free variable number in *SHELX* or the same reasonable occupancy assignment in *REFMAC*5 owing to the short distance between the two alternative conformations. Residues 155–159 that show two alternate conformations in all three structures were refined in a similar manner. The mutant crystal structures were compared with each other and also with the recently published high-resolution structure of wild-type EGFP (PDB entry 4eul; Arpino *et al.*, 2012) by superimposing their C_α atoms using *SUPERPOSE* from the *CCP*4 suite of programs (Krissinel & Henrick, 2004; Winn *et al.*, 2011). Structural figures were made using *PyMOL* (DeLano, 2002). The atomic coordinates and structure factors have been deposited in the PDB with codes 4l13, 4l1i and 4l12 for CatchER(apo), CatchER-Ca^{2+} and CatchER-Gd^{3+}, respectively.

2.3. Absorbance spectrum of CatchER and metal-binding affinity *via* fluorescence spectroscopy

The absorbance spectra of CatchER and EGFP were obtained using a Shimadzu UV-1601 spectrophotometer. Samples were prepared using 20 μM protein in 10 m*M* Tris pH 7.4. To the CatchER sample, 5 μM ethylene glycol tetraacetic acid (EGTA) was added to obtain the Ca^{2+}-free spectrum. To obtain the Ca^{2+}-loaded CatchER spectrum, 5 m*M* $CaCl_2$ was added to the sample. The absorbance spectrum of Gd^{3+}-loaded CatchER was obtained in the same manner with the addition of 200 μM $GdCl_3$ to the CatchER sample prepared in 20 m*M* PIPES pH 6.8. The fluorescence response of CatchER to Gd^{3+} and Ca^{2+} was analyzed using a Photon Technology International (PTI; Canada) spectrofluorometer. The spectra were collected with the *Felix*32 fluorescence analysis software. Slit widths were set to 0.35 mm for excitation and emission. Samples of 10 μM CatchER with 2 μM EGTA were prepared in triplicate in 20 m*M* PIPES pH 6.8 for Gd^{3+} titrations and in 10 m*M* Tris pH 7.4 for Ca^{2+} titrations. Samples were excited at 395 and 488 nm with emission recorded from 500 to 600 nm. To determine the K_d, the following 1:1 binding equation was used,

$$[PM]/[P_T] = [M_T]/K_d + [M_T],$$

where K_d is the dissociation constant, $[PM]/[P_T]$ is the fractional change of complex formation and $[M_T]$ is the total metal concentration. The equation was derived as follows

$$[P_T] = [P_F] + [PM],$$

$$[M_T] = [M_F] + [PM],$$

$$[P_F] = [P_T] - [PM],$$

$$K_d = [P_F][M_F]/[PM],$$

$$K_d = \{([P_T] - [PM])([M_F])\}/([PM]),$$

$$([PM])(K_d + [M_F]) = ([M_F][P_T]),$$

$$([PM]/[P_T]) = [M_T]/K_d + [M_T].$$

Table 2
Crystallographic data and refinement statistics for CatchER complexes.

	CatchER(apo)	CatchER-Ca^{2+}	CatchER-Gd^{3+}
X-ray source	APS 22ID	APS 22ID	APS 22BM
Wavelength (Å)	0.8	0.8	1.0
Temperature (K)	100	100	100
Space group	$C222_1$	$P2_12_12_1$	$C222_1$
Unit-cell parameters (Å)	a = 61.40, b = 88.53, c = 118.43	a = 54.24, b = 61.06, c = 67.40	a = 61.06, b = 88.33, c = 118.17
Protein molecules per asymmetric unit	1	1	1
Unique reflections	38048	70349	30260
R_{merge}† (%)	6.8 (22.8)	8.1 (39.2)	8.5 (18.5)
$\langle I/\sigma(I)\rangle$†	22.6 (7.7)	19.9 (6.1)	14.2 (8.7)
Resolution range (Å)	31.08–1.66	50–1.20	27.13–1.78
Completeness† (%)	99.1 (93.6)	99.2 (100)	98.3 (93.8)
R_{work}	0.181	0.150	0.196
R_{free}	0.203	0.191	0.219
No. of protein atoms (includes alternative conformations)	1956	1967	1922
No. of H_2O molecules (total occupancies‡)	167 (151)	197 (191.5)	138 (128.5)
No. of ions (occupancy)	1 (1.0)	2 (0.5/0.5)	2 (0.7/0.3)
R.m.s. deviation from ideality			
Bonds (Å)	0.012	0.012	0.014
Angle distance	1.527 Å§	0.031°¶	1.594 Å§
Average B factors (Å^2)			
Main-chain atoms	17.46	16.60	20.40
Side-chain atoms	19.34	20.52	22.01
H_2O	25.47	28.80	25.79
Ions	43.74	35.67	37.56
Ramachandran plots results, residues in			
Favored region	221 (98.2%)	220 (98.7%)	221 (98.2%)
Allowed region	4 (1.8%)	3 (1.3%)	4 (1.8%)

† Values in parentheses are for the highest resolution shell. ‡ Total occupancies are the sum of calculated occupancies of all the atoms or ions. § The angle r.m.s.d. in *REFMAC*5.2 is indicated by angle in degrees. ¶ The angle r.m.s.d. in *SHELX*-97 is indicated by distance in Å.

Dividing by $[P_T]$ gives the fractional saturation of the protein. Because $[M_F] = [M_T]$, we can replace $[M_F]$ with $[M_T]$.

2.4. CatchER-Gd^{3+} stoichiometry *via* Job plot

The method of continuous variations (Job plot) was used to confirm the 1:1 binding of CatchER to Gd^{3+}. Duplicate samples of 40, 35, 30, 25, 20, 15 and 10 µ*M* CatchER (the actual concentrations were 38, 35, 30, 24, 20, 15 and 10.5 µ*M* based on the absorbance at 280 nm) were prepared in 20 m*M* PIPES pH 6.8. The absorbance and fluorescence spectra of each sample were recorded before and after adding 10, 15, 20, 25, 30, 35 and 40 µ*M* Gd^{3+}, respectively, to keep the total [CatchER + Gd^{3+}] equal to 50 µ*M* (Table 1). The relative amount of Gd^{3+}-bound CatchER was calculated using the equation

$$C_b = \left(\frac{F_{Gd,bound}}{F_{Gd,free}} - 1\right) \times \frac{c}{a},$$

where C_b is the amount of CatchER bound to Gd^{3+}, $F_{Gd,bound}/F_{Gd,free}$ is the ratio of the fluorescence intensity with and without Gd^{3+}, c is the concentration of CatchER and a is a constant of the difference between the quantum yields of the bound and free forms of CatchER divided by the quantum yield of the free form. A complete derivation of this equation can be found in Tang *et al.* (2011).

3. Results and discussion

3.1. Metal-binding properties of CatchER

The absorption and fluorescence response of CatchER to Ca^{2+} and Gd^{3+} is shown in Figs. 2(*a*)–2(*f*) with the fluorescence monitored at 510 nm upon excitation at 488 nm. The normalized response shows an excellent fit to the 1:1 binding equation. Supplementary Fig. S1[1] shows the fluorescence response and normalization for Gd^{3+} and Ca^{2+} at 395 nm excitation. From these results, the K_d of CatchER for Gd^{3+} is 53.0 ± 4.0 and 177.0 ± 13.6 µ*M* when excited at 395 and 488 nm, respectively. The K_d of CatchER for Ca^{2+} was determined to be 315.4 ± 40.0 and 227.0 ± 3.3 µ*M* when excited at 395 and 488 nm, respectively. The addition of Ca^{2+} or Gd^{3+} greatly enhances the fluorescence emission of CatchER at 510 nm when excited at 395 or 488 nm.

The stoichiometric interaction of CatchER with Gd^{3+} was investigated and determined using the Job plot method (Fig. 2*f*). Supplementary Fig. S1(*c*) lists the calculated relative amounts of Gd^{3+}-loaded CatchER from the plot in Fig. 2(*f*). The largest amount of Gd^{3+}-bound CatchER was obtained at equimolar amounts of CatchER and Gd^{3+} (25 µ*M*). Thus, CatchER forms a 1:1 complex with Gd^{3+} (Table 1). In Tang *et al.* (2011), CatchER was shown to exhibit a 1:1 binding stoichiometry with Ca^{2+} as well. Overall, CatchER exhibits a 1:1 stoichiometric interaction with Gd^{3+} and Ca^{2+}.

3.2. Crystallographic analysis of CatchER structures

Crystal structures of CatchER in the apo form, Ca^{2+}-bound form and Gd^{3+}-loaded form were determined to identify and analyze the Ca^{2+}-binding site in the designed sensor. The crystallographic data-collection and refinement statistics are summarized in Table 2 and the data statistics *versus* resolution for each CatchER are listed in Supplementary Table S1. The crystal structures of CatchER(apo), CatchER-Ca^{2+} and CatchER-Gd^{3+} were refined to R factors of 18.1, 15.0 and 19.6% at resolutions of 1.66, 1.20 and 1.78 Å, respectively. These three structures belonged to two different space groups: CatchER(apo) and CatchER-Gd^{3+} belong to $C222_1$ and CatchER-Ca^{2+} belongs to $P2_12_12_1$. Structure validation was performed and the Ramachandran plots are shown in Supplementary Fig. S3. The *p*-hydroxylbenzylidene-

[1] Supplementary material has been deposited in the IUCr electronic archive (Reference: DW5059). Services for accessing this material are described at the back of the journal.

imidazolidinone chromophore (CRO66) is clearly visible in the electron density for all structures, as shown in Fig. 3(*a*) for CatchER-Ca^{2+}. The three crystal structures have very similar backbone conformations, as demonstrated by the low r.m.s.d. values of 0.09–0.20 Å for each pair of structures. Slightly more variation is seen relative to the EGFP structure (PDB entry 4eul), with r.m.s.d. values of 0.39–0.41 Å.

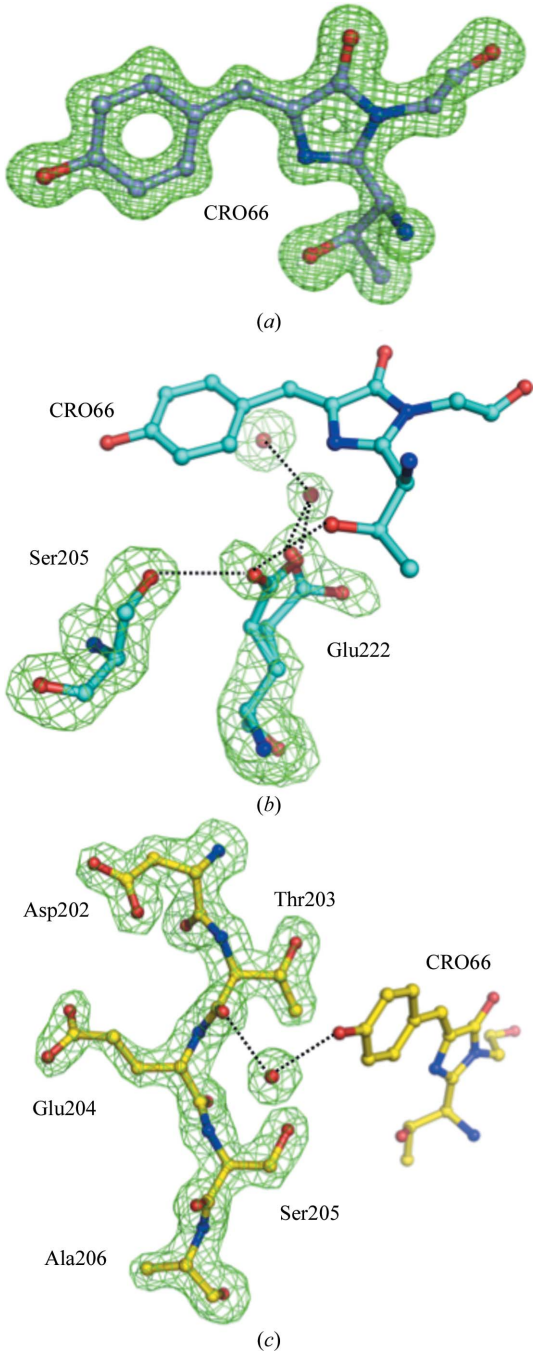

Figure 3
(*a*) $F_o - F_c$ OMIT map showing the chromophore from CatchER-Ca^{2+} contoured at 4.0σ. (*b*) $F_o - F_c$ OMIT maps showing two conformations of Glu222 from CatchER-Gd^{3+} and two water molecules contoured at 3.0σ. (*c*) $F_o - F_c$ OMIT map showing residues Asp202–Ala206 of CatchER(apo) and one water molecule contoured at 3.0σ with chromophore (CRO66). The dotted lines represent hydrogen-bond interactions.

Table 3
CatchER–metal interactions within the proposed coordination site.

(*a*) Ca^{2+}.

CatchER atom	*B* factor (Å^2)/occupancy	Distance (Å)	
		Ca^{2+}(1)	Ca^{2+}(2)
Glu147 OE2	30.76/1.0	1.9	2.1
Asp202 OD1	18.84/1.0	3.0	3.2
Asp202 OD2	27.29/1.0	2.6	2.8
H_2O1	35.36/1.0	3.1	
H_2O2	31.95/1.0	2.5	
H_2O3	25.38/1.0	1.8	
H_2O4	44.32/0.5	2.5	3.0
H_2O5	25.02/1.0		2.1
H_2O6	42.44/1.0		2.7

(*b*) Gd^{3+}.

CatchER atom	*B* factor (Å^2)/occupancy	Distance (Å)	
		Gd^{3+}(1)	Gd^{3+}(2)
Glu147 OE2	30.51/1.0	2.2	
Asp202 OD1	22.52/1.0	2.6	
Asp202 OD2	30.51/1.0	2.5	
Glu204 OE1	32.69/1.0	2.6	3.1
Glu204 OE2	29.53/1.0		3.1
H_2O1	33.89/1.0	2.1	
H_2O2	24.74/1.0		2.3
H_2O3	33.62/1.0		2.9

Because of the high resolution of the diffraction data, the solvent was fitted with 167 water molecules for CatchER(apo), 197 water molecules for CatchER-Ca^{2+} and 138 water molecules for CatchER-Gd^{3+}. One acetate molecule was refined with an occupancy of 1.0 in CatchER(apo), two Ca^{2+} ions with relative occupancy of 0.5 each in CatchER-Ca^{2+} and two Gd^{3+} ions with relative occupancies of 0.7 and 0.3 in CatchER-Gd^{3+}. These molecules were identified by the shape and peak height in the electron-density maps, *B* factors and potential interactions with other molecules, as described in the next section. The occupancies were calculated with *SHELX* for CatchER-Ca^{2+} and were estimated with *REFMAC*5 for the other structures.

Alternative conformations were modeled for a total of 19, 23 and 13 residues in the CatchER(apo), CatchER-Ca^{2+} and CatchER-Gd^{3+} structures, respectively. The surface loop of residues 155–159 shows two alternative conformations with about 0.5/0.5 relative occupancy in all three structures (Supplementary Fig. S2), while most other reported structures have a single conformation of these residues. This disordered loop is located on the opposite side of the protein to the designed metal-binding site. Notably, Glu222 consistently shows two alternate conformations in the CatchER-Ca^{2+} and CatchER-Gd^{3+} structures (Fig. 3*b*) and a single conformation in CatchER(apo). Among the five designed mutations located on three neighboring β-strands, the side chain of Glu225 has two alternate conformations in CatchER(apo) and CatchER-Ca^{2+} that interact with the two alternative conformations of the Arg73 side chain. Owing to the surface location of the five mutated residues and the potential for radiation damage to the carboxylate side chains, Glu204, Glu223 and Glu225

showed relatively poor electron density in the different CatchER complexes.

3.3. Identification of metal ions in the designed binding site of CatchER

CatchER was designed with five mutated residues, S147E, S202D, Q204E, F223E and T225E, compared with EGFP. The mutations are located on three β-strands, pointing out of the protein β-barrel to form a penta-carboxylate ionic environment suitable for binding Ca^{2+} (Fig. 1). In CatchER(apo), one of the carboxyl O atoms of Glu147 forms close interactions with the carboxylate of Asp202, suggesting possible protonation of the carboxylates (Fig. 4*a*). Protonated carboxylates have been reported in other protein crystal structures (Tie *et al.*, 2005). The Glu147 and Asp202 carboxylates are further apart with no direct interaction in the CatchER structures with Ca^{2+} and Gd^{3+}, and additional solvent peaks were observed in this region of the electron-density maps.

The identification of Ca^{2+} in the designed binding site of CatchER was not trivial partly because of the fast off-rate related to its weak calcium-binding affinity. Crystals of CatchER were grown in high concentrations of 50 m*M* Ca^{2+} to ensure saturation of the CatchER molecules; however, the nonprotein peaks in the electron-density maps near the mutated residues were indistinguishable from those assigned to water elsewhere (Fig. 4*b*). Therefore, the presence of Ca^{2+} was deduced from the interactions with nearby protein residues and water molecules. Two possible locations for Ca^{2+} were identified, mostly by the presence of shorter distances of 1.8–2.5 Å to interacting O atoms of Glu147 and water molecules and further interactions with Asp202 and other water molecules in the designed site (Fig. 4*b*; Table 3). These interatomic distances are within the range observed in high-resolution crystal structures of proteins (Harding, 2001). The two locations were fitted with Ca^{2+} ions refined at partial occupancy (0.5/0.5). However, this deduction for Ca^{2+} cannot exclude the possible binding of Na^{+} or water molecules from the crystallization solution. No significant electron density was present in the apo structure at the positions assigned to Ca^{2+} near Glu147 and Asp202.

In order to pinpoint the metal-binding site more definitively, the structure of CatchER-Gd^{3+} was obtained from apo crystals soaked in high concentrations of $GdCl_3$. Ca^{2+} has 18 electrons orbiting the nucleus, while Gd^{3+} has 61 orbital electrons. Therefore, it is easier to locate Gd^{3+} with increased diffraction over Ca^{2+} since the X-ray atomic scattering factor increases with atomic number. The major 0.7 occupancy Gd^{3+} ion was identified unambiguously from the very high peak at 22σ in the electron density indicative of a heavy-metal ion (Fig. 4*c*). This Gd^{3+} ion is located between the side chains of Glu147, Asp202 and Glu204, forming four ionic interactions with these three residues at distances of 2.2, 2.5, 2.6 and 2.6 Å and one with a nearby water molecule at 2.1 Å (Fig. 4*c* and Table 3). The second Gd^{3+} ion with 0.3 occupancy was deduced from positive difference density observed in ($F_o - F_c$) maps when a water molecule or a partial occupancy Na^{+} ion was refined at this site. Overall, the Gd^{3+} ions coordinate with the side chains of residues Glu147, Asp202 and

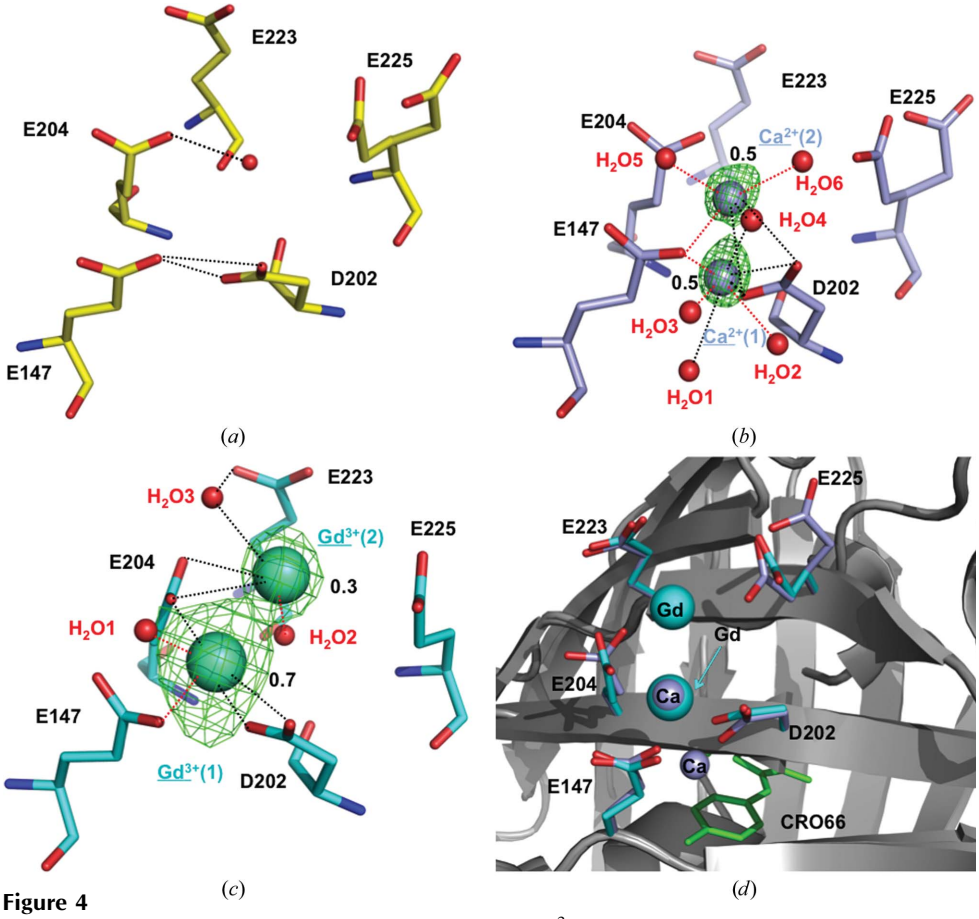

Figure 4
(*a*–*c*) The hydrogen-bond interactions at the designed Ca^{2+}-binding site for CatchER structures. The protein is represented as yellow, light blue and cyan sticks in CatchER(apo), CatchER-Ca^{2+} and CatchER-Gd^{3+}, respectively. Ca^{2+}, Gd^{3+} and water molecules are represented as spheres. The numbers (0.5/0.5, 0.7/0.3) give the relative occupancy of the alternate positions of the Ca^{2+} and Gd^{3+} ions, respectively. The interatomic (non-H) distance range of 2.6–3.2 Å was used for hydrogen bonds (black dotted lines). Shorter distances in the range 2.0–2.4 Å (red dotted lines) suggest coordination to a metal ion. The coordinating waters are numbered as in Table 3. (*d*) Superposition of CatchER-Ca^{2+} and CatchER-Gd^{3+}; the protein backbones are shown as gray cartoons and the chromophore (CRO66) is represented as green sticks. The five mutated residues and ions are shown in sticks and spheres in light blue for CatchER-Ca^{2+} and cyan for CatchER-Gd^{3+}. The cyan arrow points to the major site for Gd^{3+}.

Glu204 of the designed Ca^{2+}-binding site as well as the water molecules.

Superposition of the CatchER-Ca^{2+} and CatchER-Gd^{3+} structures revealed that the major occupancy site for the Gd^{3+} ion is identical to one of the sites deduced for the Ca^{2+} ion (Fig. 4*d*). This Ca^{2+} ion coordinates with the side chains of Glu147 and Asp202 and three water molecules. No Gd^{3+} ion was visible at the other site, where the Ca^{2+} ion coordinates with the carboxylate side chains of Glu147 and Asp202 and four water molecules (Fig. 4*b*). It is possible that the presence of the high-occupancy Gd^{3+} ion at the adjacent site precludes binding to the inner site occupied by a Ca^{2+} ion in the CatchER-Ca^{2+} structure.

The extended binding site formed by the carboxylate side chains of the mutated residues Glu147, Asp202, Glu204, Glu223 and Glu225 traps metal ions at three possible positions, as shown by superposition of CatchER-Ca^{2+} and CatchER-Gd^{3+} (Fig. 4*d*). The metal ions mainly interact with side chains of Glu147, Asp202 and Glu204. No direct interactions of designed metal-ligand residues Glu223 and Glu225 with the metal ions are visible and their side chains are not well defined in the electron-density maps, possibly owing to radiation damage. Nevertheless, both Ca^{2+} and Gd^{3+} ions are well situated at the designed Ca^{2+}-binding site in CatchER, which suggests that these X-ray structures provide snapshots of steps in the likely dynamic metal-binding process.

3.4. Structural changes around the chromophore

The chromophore interactions were compared in the CatchER structures, EGFP (PDB entry 4eul; Arpino *et al.*, 2012) and GFP (PDB entry 1emb; Brejc *et al.*, 1997). The chromophore is buried centrally in the protein molecule and is well protected from solvent. It can exist as neutral and anionic forms, which are responsible for the absorbance at 395 and 475 nm, respectively (Yang *et al.*, 1996; Fig. 5). The spectroscopic characterization of CatchER and its response to Ca^{2+} shows two absorption maxima with a major peak at 398 nm and a smaller peak at 490 nm; it thus resembles GFP with two similar excitation wavelengths, unlike EGFP with one single excitation peak at 488 nm (Tsien, 1998; Fig. 2*e*). Comparisons of the chromophore environment in the three CatchER structures and the currently solved EGFP and GFP structures have shed light on the relationship between the spectroscopic properties and the structures. The intricate hydrogen-bond networks around the chromophores of CatchER(apo), CatchER-Ca^{2+} or CatchER-Gd^{3+}, EGFP and GFP are shown in Figs. 6(*a*)–6(*d*) (Arpino *et al.*, 2012; Brejc *et al.*, 1997). Most hydrogen-bond interactions are conserved in the vicinity of the carbonyl group of the imidazolidinone ring of the chromophore (Arpino *et al.*, 2012; Brejc *et al.*, 1997; Ormö *et al.*, 1996). Two residues, Thr203 and Glu222, show a critical role in the chemical environment of the chromophore. Thr203 has been observed with two different conformations: in one the side chain of Thr203 can make direct contact with the tyrosyl group of the chromophore, while in the other the side chain of Thr203 rotates away from the tyrosyl group and the main chain moves towards the chromophore, resulting in the elimination of direct hydrogen-bond interactions but permitting a water-mediated interaction between the main-chain carbonyl group and the chromophore tyrosyl group. In addition, the side chain of Glu222 has shown two alternate conformations in some EGFP structures (Royant & Noirclerc-Savoye, 2011; Arpino *et al.*, 2012).

In our structural analysis and comparisons, CatchER-Ca^{2+} and CatchER-Gd^{3+} have similar interactions around the chromophore, as shown schematically in Fig. 6(*b*), while CatchER(apo) has different interactions for Glu222 (Fig. 6*a*). In all three of the CatchER structures Thr203 formed a water-mediated hydrogen bond with the chromophore tyrosyl *via* the second type of conformation mentioned above. The representative OMIT map of Asp202–Asp206 adjacent to CRO66 and the mediating water for a hydrogen bond in CatchER(apo) is shown in Fig. 3(*c*). This type of interaction between the carbonyl group of Thr203 and chromophore was also found in the GFP structure (PDB entry 1emb; Fig. 6*d*), even though it also has an alternate side-chain conformation with 0.15 occupancy which can form direct hydrogen bonding to the chromophore (Brejc *et al.*, 1997). In contrast, in the EGFP structure (PDB entry 4eul) Thr203 only forms the first type of interaction (Fig. 6*c*).

Regarding the side chain of Glu222, the conformational population differs in the three CatchER structures: only one conformation of Glu222 was observed in CatchER(apo) and its side chain is considered to be deprotonated and forms a hydrogen bond to Ser205 and another to the hydroxyl group of the chromophore (Fig. 6*a*); in CatchER-Ca^{2+} and CatchER-Gd^{3+} one additional alternative conformation of Glu222 was determined which lacks interactions with the chromophore; instead, it participates in interactions with a network of water molecules linking to Gln69 (Fig. 6*b*). Recent crystallographic study of EGFP has revealed two alternate conformations for Glu222 not only in the EGFP structure (PDB entry 4eul) used here for comparison but in another reported structure (PDB entry 2y0g; Royant & Noirclerc-Savoye, 2011). In both published structures Glu222 shows similar interactions with the chromophore and the surrounding environment as in Fig. 6(*c*), which is quite similar to the arrangement in CatchER-Ca^{2+} and CatchER-Gd^{3+}. However, in the GFP structure (PDB entry 1emb), one conformation of Gly222 was defined that forms hydrogen-bond interactions as in CatchER(apo).

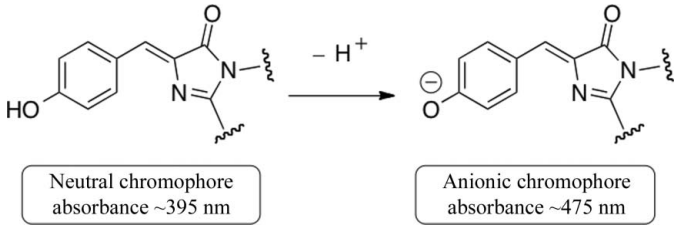

Figure 5
Protonation states of the GFP chromophore with the corresponding absorbance wavelengths.

Previously, profound but opposite effects of residues Thr203 and Glu222 were reported from mutagenesis and analysis of crystal structures (Heim *et al.*, 1994; Ehrig *et al.*, 1995; Brejc *et al.*, 1997). Introduction of a T203I mutation in GFP retains the 395 nm peak but eliminates the 475 nm peak, whereas GFP with an E222G mutation retains the 475 nm peak but lacks the 395 nm peak (Heim *et al.*, 1994; Ehrig *et al.*, 1995). The crystal structures of GFP and EGFP revealed that the side chain of Thr203 can stabilize a negative charge on the chromophore (anionic form chromophore) as a hydrogen-bond donor through a direct hydrogen bond to the chromophore tyrosyl residue, but the carboxylate of charged Glu222 can maintain the neutral form of the chromophore through electrostatic repulsion and the hydrogen-bonding network *via* water and Ser205 (Brejc *et al.*, 1997). In the CatchER structures the conformation of Thr203 preferred the proposed protonated form of the chromophore. The hydrogen-bond network *via* water and Ser205 is achieved by one conformation of Glu222 in deprotonated or negatively charged states and helps to maintain the neutral form of the chromophore. In CatchER-Ca^{2+} and CatchER-Gd^{3+}, even though the other conformation of Glu222 does not interact with the chromophore threonine as in EGFP (Ormo *et al.*, 1996; Royant & Noirclerc-Savoye, 2011; Arpino *et al.*, 2012), this alternate conformation with almost half occupancy is proposed to be protonated and can no longer maintain the neutral form of the chromophore. Therefore, although there is only one conformation of Glu222 in CatchER(apo), we suggest that the

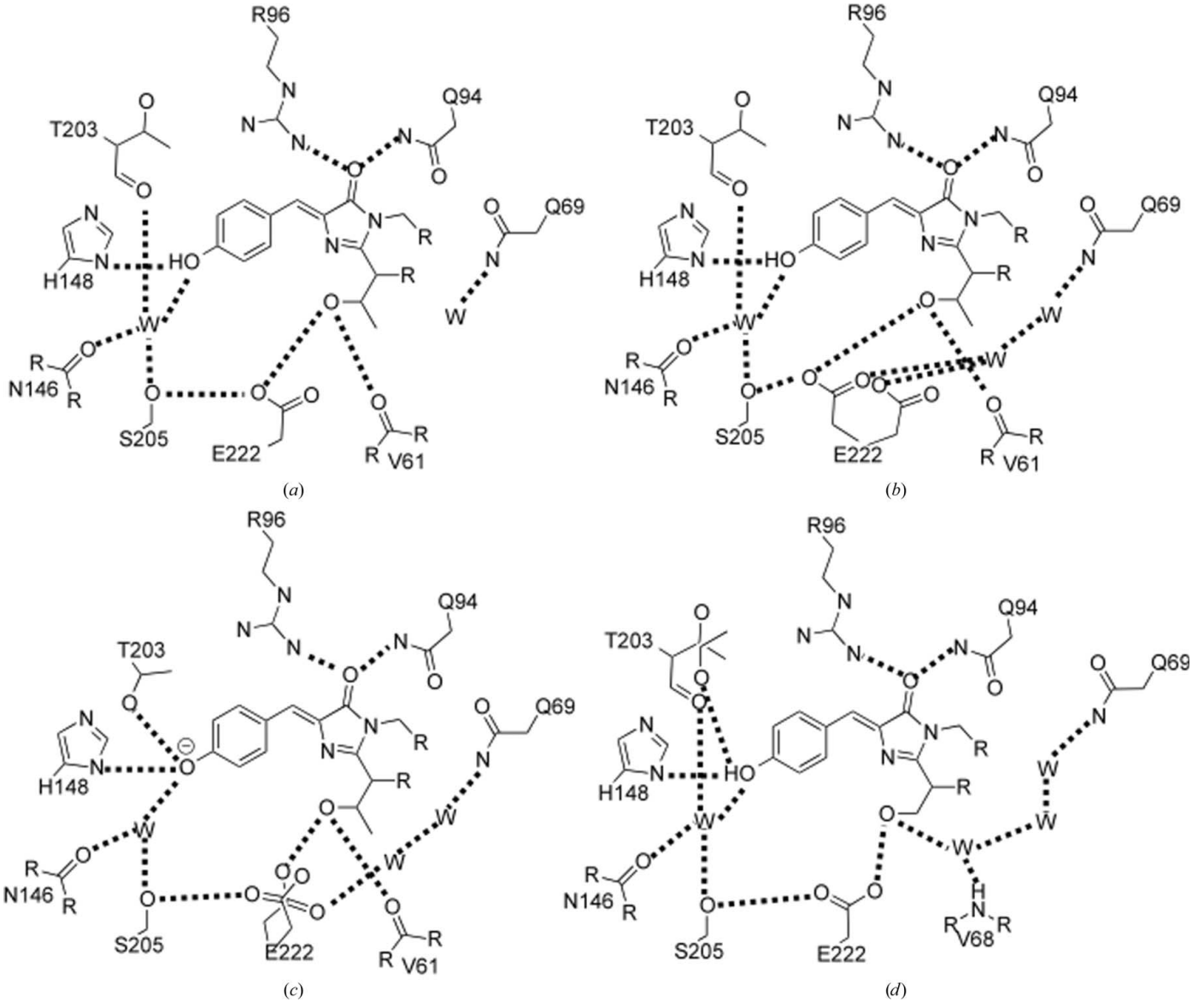

Figure 6
Scheme of the hydrogen-bond interactions between the chromophore and surrounding residues and water molecules (W) in CatchER(apo) (*a*), CatchER-Ca^{2+} or Gd^{3+} (*b*), EGFP (*c*) and GFP (*d*). Hydrogen bonds are shown as dashed lines. The interatomic (non-H) distance range of 2.6–3.2 Å was used for hydrogen bonds.

chromophore of CatchER has a mixture of neutral and negatively charged states, as observed in wild-type GFP, which has two conformations of Thr203 (Brejc *et al.*, 1997).

The ratio of neutral and negatively charged chromophore can differ in the CatchER structures based on their spectroscopic properties. In the absorbance spectra, addition of Ca^{2+} results in a concurrent increased intensity around 490 nm (increase in deprotonated chromophore) and a decreased absorption intensity around 398 nm (decrease in the protonated chromophore state), exhibiting an optical spectral feature that more closely resembles that of EGFP, as shown in Fig. 2(*a*). Tang and coworkers also reported that the presence of calcium results in a decrease in the pK_a value of the chromophore of CatchER (Tang *et al.*, 2011), suggesting that the chromophore in CatchER is more deprotonated upon calcium binding. This change could be related to the observed equilibrium shift in conformational populations of Glu222 in CatchER: the increase of deprotonated chromophore on calcium binding is likely to be owing to the stabilizing capability of Glu222 as a hydrogen-bond donor with the hydrogen-bond acceptor of deprotonated Thr65 in the chromophore (Fig. 6*b*). Such a stabilizing effect is manifested by the changes in the proton wire network between apo and calcium-loaded forms of CatchER and EGFP, as shown in Figs. 6(*a*)–6(*c*). Thus, binding of calcium induces an equilibrium shift in conformational populations of the Glu222 side chain and its network of interactions through two water molecules to Gln69. Overall, the crystal structures of CatchER have reinforced support for the proposed excited-state photon-transfer pathway for the photoisomerization of GFP which was based on structural and spectroscopic studies (Chattoraj *et al.*, 1996; Brejc *et al.*, 1997). A similar observation and proposed interpretation apply to Gd^{3+}-induced change (Fig. 2*b* and Fig. 6*b*).

No significant difference was observed for Leu42, Thr43, Tyr143 and Thr153 in the structural comparison of CatchER(apo) with CatchER-Ca^{2+}, despite the chemical shift changes related to Ca^{2+} binding (Tang *et al.*, 2011) shown in dynamic NMR. The addition of Ca^{2+} leads to the gradual splitting of one resonance into two for Gln69, which is buried inside the protein (Tang *et al.*, 2011). In both CatchER-Ca^{2+} and CatchER-Gd^{3+}, Gln69 forms a hydrogen-bond network through two water molecules with Glu222 and this network was also found in EGFP (PDB entry 4eul; Fig. 6*b*). However, this network was interrupted owing to a missing water molecule in CatchER(apo) (Fig. 6*a*). Therefore, we propose here that the calcium-induced change in optical properties could also be associated with the Gln69 hydrogen-bond network.

3.5. Relationship between mutations of the novel metal-binding site and optical properties

CatchER was selected from a series of Ca^{2+} sensors designed by introducing different mutations around the desired Ca^{2+}-binding site, designated D8, D9, D10, D11 (CatchER) and D12 (Tang *et al.*, 2011). These mutants all show an increase in the peak at 398 nm and a decrease at 490 nm to different extents. D8 contains only two mutations, S202D and F223E, while the other variants have additional mutations, which indicated that the S202D and/or F223E mutations might play an important role in the conserved absorbance changes for the designed proteins. Based on the structural changes around the chromophore, Thr203 and Glu222 are two key residues that account for the altered chemical environment of the chromophore. The effects of these two residues might be modified by mutations of adjacent residues: S202D and F223E. However, the F223E mutation makes no direct interaction with Ca^{2+} in CatchER-Ca^{2+}, although it forms a water-mediated hydrogen bond with one Gd^{3+} in the CatchER-Gd^{3+} structure. Instead, the S147E mutation appears to function as the anion for interacting with metal cations, while the S202D mutation is also involved in metal coordination based on our crystal structures. The main chain of residues 202–206 has shifted by 0.7–0.9 Å in association with the rotation of Thr203 in CatchER relative to EGFP, which leads to the ionization change of the chromophore (Fig. 7).

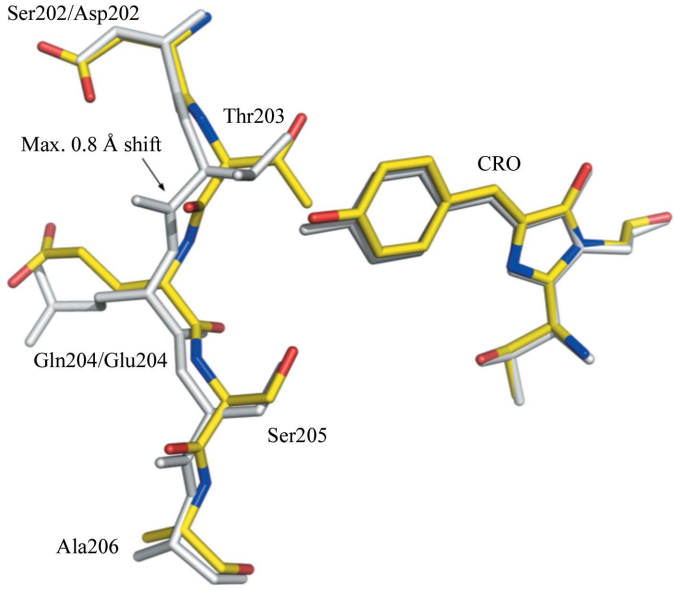

Figure 7
Comparison of EGFP and CatchER(apo) at the chromophore and nearby residues. Residues 202–206 of EGFP and CatchER(apo) are shown as sticks in gray and yellow, respectively. Ser202/Asp202 and Gln204/Glu204 label mutated residues in EGFP/CatchER(apo). The main chain from residues 202–206 shifts with a maximum value of 0.8 Å as indicated by the arrow.

4. Conclusions

The binding of the metal ions Ca^{2+} and Gd^{3+} to the designed calcium sensor CatchER has been investigated by spectroscopic methods and X-ray crystallography. Both the kinetic assays and the structures demonstrated the binding of the two types of metal ions to CatchER; however, there were unexpected differences. The crystal structures of CatchER in the apo form and in its complexes with Ca^{2+} and Gd^{3+} reveal snapshots of the dynamic binding of metal ions to the designed

site comprising five carboxylate side chains. Both Ca^{2+} and Gd^{3+} ions were observed in two locations within the designed binding site. The high (millimolar) concentrations of Ca^{2+} and Gd^{3+} used to obtain the crystal structures of their CatchER complexes resulted in two alternative binding sites for each metal ion with one central common binding site. In solution, however, these two metal ions bind CatchER with a 1:1 stoichiometry and micromolar affinity. These structures suggest that the ability of Ca^{2+} ions to jump between two possible binding sites may be partly responsible for the fast kinetics of metal-ion binding to CatchER.

We thank Drs Johnson Agniswamy, Yanyi Chen and Huiming Li and Malcolm Degrado for valuable discussions. Data were collected at the Southeast Regional Collaborative Access Team (SER-CAT) beamline at the Advanced Photon Source, Argonne National Laboratory. Supporting institutions may be found at http://www.ser-cat.org/members.html. Use of the Advanced Photon Source was supported by the US Department of Energy, Office of Science, Office of Basic Energy Sciences under Contract No. W-31-109-Eng-38. This work was supported, in part, by NIH grants GM081749 NIH and EB007268 to JJY, by a seed grant from Georgia State University Brains and Behavior Area of Focus, by a University Doctoral Fellowship in Diagnostics and Therapy fellowship (YZ) and by Brains and Behavior graduate fellowships to ST and YZ.

References

Arpino, J. A., Rizkallah, P. J. & Jones, D. D. (2012). *PLoS One*, **7**, e47132.

Baird, G. S., Zacharias, D. A. & Tsien, R. Y. (1999). *Proc. Natl Acad. Sci. USA*, **96**, 11241–11246.

Berridge, M. J. (1998). *Neuron*, **21**, 13–26.

Berridge, M. J., Bootman, M. D. & Lipp, P. (1998). *Nature (London)*, **395**, 645–648.

Bers, D. M. & Guo, T. (2005). *Ann. N. Y. Acad. Sci.* **1047**, 86–98.

Brejc, K., Sixma, T. K., Kitts, P. A., Kain, S. R., Tsien, R. Y., Ormö, M. & Remington, S. J. (1997). *Proc. Natl Acad. Sci. USA*, **94**, 2306–2311.

Chapleau, R. R., Blomberg, R., Ford, P. C. & Sagermann, M. (2008). *Protein Sci.* **17**, 614–622.

Chattoraj, M., King, B. A., Bublitz, G. U. & Boxer, S. G. (1996). *Proc. Natl Acad. Sci. USA*, **93**, 8362–8367.

DeLano, W. L. (2002). *PyMOL*. http://www.pymol.org.

Ehrig, T., O'Kane, D. J. & Prendergast, F. G. (1995). *FEBS Lett.* **367**, 163–166.

Emsley, P. & Cowtan, K. (2004). *Acta Cryst.* D**60**, 2126–2132.

Evanko, D. S. & Haydon, P. G. (2005). *Cell Calcium*, **37**, 341–348.

Harding, M. M. (2001). *Acta Cryst.* D**57**, 401–411.

Heim, R., Prasher, D. C. & Tsien, R. Y. (1994). *Proc. Natl Acad. Sci. USA*, **91**, 12501–12504.

Jiménez-Moreno, R., Wang, Z.-M., Messi, M. L. & Delbono, O. (2010). *Pflugers Arch.* **459**, 725–735.

Krissinel, E. & Henrick, K. (2004). *Acta Cryst.* D**60**, 2256–2268.

Mank, M., Reiff, D. F., Heim, N., Friedrich, M. W., Borst, A. & Griesbeck, O. (2006). *Biophys. J.* **90**, 1790–1796.

Mank, M., Santos, A. F., Direnberger, S., Mrsic Flogel, T. D., Hofer, S. B., Stein, V., Hendel, T., Reiff, D. F., Levelt, C., Borst, A., Bonhoeffer, T., Hübener, M. & Griesbeck, O. (2008). *Nature Methods*, **5**, 805–811.

Miyawaki, A., Griesbeck, O., Heim, R. & Tsien, R. Y. (1999). *Proc. Natl Acad. Sci. USA*, **96**, 2135–2140.

Miyawaki, A., Llopis, J., Heim, R., McCaffery, J. M., Adams, J. A., Ikura, M. & Tsien, R. Y. (1997). *Nature (London)*, **388**, 882–887.

Murshudov, G. N., Skubák, P., Lebedev, A. A., Pannu, N. S., Steiner, R. A., Nicholls, R. A., Winn, M. D., Long, F. & Vagin, A. A. (2011). *Acta Cryst.* D**67**, 355–367.

Nagai, T., Sawano, A., Park, E. S. & Miyawaki, A. (2001). *Proc. Natl Acad. Sci. USA*, **98**, 3197–3202.

Ohkura, M., Matsuzaki, M., Kasai, H., Imoto, K. & Nakai, J. (2005). *Anal. Chem.* **77**, 5861–5869.

Ormö, M., Cubitt, A. B., Kallio, K., Gross, L. A., Tsien, R. Y. & Remington, S. J. (1996). *Science*, **273**, 1392–1395.

Otwinowski, Z. & Minor, W. (1997). *Methods Enzymol.* **267**, 307–326.

Palmer, A. E., Giacomello, M., Kortemme, T., Hires, S. A., Lev-Ram, V., Baker, D. & Tsien, R. Y. (2006). *Chem. Biol.* **13**, 521–530.

Palmer, A. E., Jin, C., Reed, J. C. & Tsien, R. Y. (2004). *Proc. Natl Acad. Sci. USA*, **101**, 17404–17409.

Persechini, A., Lynch, J. A. & Romoser, V. A. (1997). *Cell Calcium*, **22**, 209–216.

Romoser, V. A., Hinkle, P. M. & Persechini, A. (1997). *J. Biol. Chem.* **272**, 13270–13274.

Royant, A. & Noirclerc-Savoye, M. (2011). *J. Struct. Biol.* **174**, 385–390.

Rudolf, R., Magalhães, P. J. & Pozzan, T. (2006). *J. Cell Biol.* **173**, 187–193.

Sheldrick, G. M. (2008). *Acta Cryst.* A**64**, 112–122.

Sheldrick, G. M. & Schneider, T. R. (1997). *Methods Enzymol.* **277**, 319–343.

Solovyova, N. & Verkhratsky, A. (2002). *J. Neurosci. Methods*, **122**, 1–12.

Takahashi, A., Camacho, P., Lechleiter, J. D. & Herman, B. (1999). *Physiol. Rev.* **79**, 1089–1125.

Tang, S., Wong, H.-C., Wang, Z.-M., Huang, Y., Zou, J., Zhuo, Y., Pennati, A., Gadda, G., Delbono, O. & Yang, J. J. (2011). *Proc. Natl Acad. Sci. USA*, **108**, 16265–16270.

Tie, Y., Boross, P. I., Wang, Y.-F., Gaddis, L., Liu, F., Chen, X., Tozser, J., Harrison, R. W. & Weber, I. T. (2005). *FEBS J.* **272**, 5265–5277.

Tsien, R. Y. (1998). *Annu. Rev. Biochem.* **67**, 509–544.

Vagin, A. & Teplyakov, A. (2010). *Acta Cryst.* D**66**, 22–25.

Wang, Z.-M., Tang, S., Messi, M. L., Yang, J. J. & Delbono, O. (2012). *Pflugers Arch.* **463**, 615–624.

Winn, M. D. *et al.* (2011). *Acta Cryst.* D**67**, 235–242.

Yang, F., Moss, L. G. & Phillips, G. N. (1996). *Nature Biotechnol.* **14**, 1246–1251.

Zhang, X. & Joseph, S. K. (2001). *Biochem. J.* **360**, 395–400.

Zou, J., Hofer, A. M., Lurtz, M. M., Gadda, G., Ellis, A. L., Chen, N., Huang, Y., Holder, A., Ye, Y., Louis, C. F., Welshhans, K., Rehder, V. & Yang, J. J. (2007). *Biochemistry*, **46**, 12275–12288.